

# Cascaded Video Generation for Videos In-the-Wild

Lluís Castrejon

Université de Montréal - Mila Quebec  
Email: lluis.castrejon@gmail.com

Nicolas Ballas

Facebook AI Research  
Email: ballasn@fb.com

Aaron Courville

Université de Montréal - Mila Quebec - CIFAR AI Chair  
Email: aaron.courville@umontreal.ca

**Abstract**—Videos can be created by first outlining a global view of the scene and then adding local details. Inspired by this idea we propose a cascaded model for video generation which follows a coarse to fine approach. First our model generates a low resolution video, establishing the global scene structure, which is then refined by subsequent cascade levels operating at larger resolutions. We train each cascade level sequentially on partial views of the videos, which reduces the computational complexity of our model and makes it scalable to high-resolution videos with many frames. We empirically validate our approach on UCF101 and Kinetics-600, for which our model is competitive with the state-of-the-art. We further demonstrate the scaling capabilities of our model and train a three-level model on the BDD100K dataset which generates 256x256 pixels videos with 48 frames.

## I. INTRODUCTION

Humans have the ability to simulate visual objects and their dynamics using their imagination. This ability is linked to the ability to perform temporal planning or counter-factual thinking. Replicating this ability in machines is a longstanding challenge that generative models try to address. Advances in generative modeling and increased computational resources have enabled the generation of realistic high-resolution images [1] or coherent text in documents [2]. Yet, video generation models have been less successful, in part due to their high memory requirements that scale with the generation resolution and length.

When creating visual data, artists often first produce a rough outline of the scene, to which then they add local details in multiple iterations [3]. The outline ensures global scene consistency and divides the creative process into multiple tractable local steps. Inspired by this process we propose CVG, a cascaded video generation model which divides the generative process into a set of simpler problems. CVG first generates a rough video that depicts a scene at a reduced framerate and resolution. This scene outline is then progressively upscaled and temporally interpolated to obtain the desired final video by one or more upscaling levels as depicted in Figure 1. Every cascade level outputs a video that serves as the input to the next one, with each level specializing in a particular aspect of the generation.

Levels in our model are trained greedily, i.e. in sequence and not end-to-end. This allows to train only one level at a time and thus reduce the overall training memory requirements. We formulate each level as an adversarial game that we solve leveraging the GAN framework. Our training setup has the same global solution as an end-to-end model.

To further reduce the computational needs of our model, upscaling cascade levels can be applied only on temporal crops

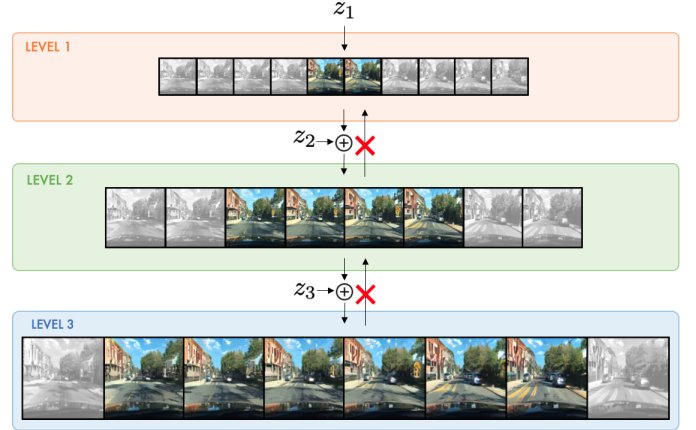


**Fig. 1: Cascaded Video Generation** We propose to divide the generative process into multiple simpler problems. CVG first generates a low resolution video that depicts a full scene at a reduced framerate. This scene outline is then progressively upscaled and temporally interpolated. Levels are trained sequentially and do not backpropagate gradient to previous levels. Additionally, upscaling levels can be trained on temporal crops of previous level outputs (illustrated by the non-shaded images) to reduce their computational requirements. Our model outperforms or matches the state-of-the-art in video generation and enables the generation of longer high resolution videos due to better scaling properties than previous methods.

from previous outputs during training. Despite this temporally-local training, upscaling levels are capable of producing videos with temporal coherence at inference time, as they upscale the output of the first level, which is temporally complete albeit at a reduced resolution. This makes CVG more scalable than previous methods, making it capable of generating high resolution videos with a larger number of frames.

Our contributions can be summarized as follows:

- We define a cascade model for video generation which divides the generation process into multiple tractable steps.
- We empirically validate our approach on UCF101, Kinetics-600 and BDD100K, large-scale datasets with complex videos in real-world scenarios. CVG matches or outperforms the state-of-the-art video generation models on these datasets.
- We demonstrate that our approach has better scaling properties than comparable non-cascaded approaches and train a three-level model to generate videos with 48 frames at a resolution of 256x256 pixels.

## II. CASCADED VIDEO GENERATION

Video scenes can be created by first outlining the global scene and then adding local details. Following this intuition we propose CVG, a cascade model in which each level only treats a lower dimensional view of the data. Video generation models struggle to scale to high frame resolutions and long temporal ranges. The goal of our method is to break down the generation process into smaller steps which require less computational resources when considered independently.

**Problem Setting** We consider a dataset of videos  $(\mathbf{x}_1, \dots, \mathbf{x}_n)$  where each video  $\mathbf{x}_i = (\mathbf{x}_{i;0}, \dots, \mathbf{x}_{i;T})$  is a sequence of  $T$  frames  $\mathbf{x}_{i;t} \in \mathbb{R}^{H \times W \times 3}$ . Let  $f_s$  denote a spatial bilinear downsampling operator and  $f_t$  a temporal subsampling operator. For each video  $\mathbf{x}_i$ , we can obtain lower resolution views of our video by repeated application of  $f_s$  and  $f_t$ , i.e.  $\mathbf{x}_i^l = f_s(f_t(\mathbf{x}_i^{l+1}), \forall l \in [1..L])$  with  $\mathbf{x}_i^L = \mathbf{x}_i$ .

Each  $(\mathbf{x}_i^1, \dots, \mathbf{x}_i^L)$  comes from a joint data distribution  $p_d$ . The task of video generation consists in learning a generative distribution  $p_g$  such that  $p_g = p_d$ .

**Cascaded Generative Model** We define a generative model that approximates the joint data distribution according to the following factorization:

$$p_g(\mathbf{x}^1, \dots, \mathbf{x}^L) = p_{g_L}(\mathbf{x}^L | \mathbf{x}^{L-1}) \dots p_{g_2}(\mathbf{x}^2 | \mathbf{x}^1) p_{g_1}(\mathbf{x}^1). \quad (1)$$

Each  $p_{g_i}$  defines a level in our model. This formulation allows us to decompose the generative process into a set of smaller problems. The first level  $p_{g_1}$  produces low resolution and temporally subsampled videos from a latent variable. For subsampling factors  $K_T$  and  $K_S$  (for time and space respectively), the initial level generates videos  $\mathbf{x}_i^1 = (\mathbf{x}_{i;0}^1, \mathbf{x}_{i;K_T}^1, \mathbf{x}_{i;2K_T}^1, \dots, \mathbf{x}_{i;T}^1)$ , which is a sequence of  $\frac{T}{K_T}$  frames  $\mathbf{x}_{i;t}^1 \in \mathbb{R}^{\frac{H}{K_S} \times \frac{W}{K_S} \times 3}$ . The output of the first level is spatially upsampled and temporally interpolated by one or more subsequent upscaling levels.

**Training** We train our model greedily one level at a time and in order, i.e. we train the first level to generate global but downsampled videos, and then we train upscaling stages on previous level outputs one after each other. We do not train the levels in an end-to-end fashion, which allows us to break down the computation into tractable steps by only training one level at a time. We formulate a GAN objective for each stage of our model. We consider the distribution  $p_{g_l}$  in eq. 1 and solve a min-max game with the following value function:

$$\mathbb{E}_{\mathbf{x}^1 \sim p_d} [\log(D_1(\mathbf{x}^1))] + \mathbb{E}_{\mathbf{z}_1 \sim p_{z_1}} [\log(1 - D_1(G_1(\mathbf{z}_1)))], \quad (2)$$

where  $G_1$  and  $D_1$  are the generator/discriminator associated with the first stage and  $p_{z_1}$  is a noise distribution. This is the standard GAN objective [4]. For upscaling levels corresponding to  $p_{g_l}$ ,  $l > 1$ , we consider the following value function:

$$\mathbb{E}_{\mathbf{x}^{l-1}, \dots, \mathbf{x}^1 \sim p_d} \mathbb{E}_{\mathbf{x}^l \sim p_d(\cdot | \mathbf{x}^{l-1}, \dots, \mathbf{x}^1)} [\log(D_l(\mathbf{x}^l, \mathbf{x}^{l-1}))] + \mathbb{E}_{\hat{\mathbf{x}}^{l-1} \sim p_{g_{l-1}}} \mathbb{E}_{\mathbf{z}_l \sim p_{z_l}} [\log(1 - D_l(G_l(\mathbf{z}_l, \hat{\mathbf{x}}^{l-1}), \hat{\mathbf{x}}^{l-1}))], \quad (3)$$

where  $G_l$ ,  $D_l$  are the generator and discriminator of the current level and  $p_{g_{l-1}}$  is the generative distribution of the level  $l-1$ .

The min-max game associated with this value function has a global minimum when the two joint distributions are equal,  $p_d(\mathbf{x}, \dots, \mathbf{x}^l) = p_{g_l}(\mathbf{x}^l | \mathbf{x}^{l-1}) \dots p_{g_1}(\mathbf{x}^1)$  [5], [6]. We also see from eq. 3 that the discriminator for upscaling stages operates on pairs  $(\mathbf{x}^l, \mathbf{x}^{l-1})$  videos to determine whether they are real or fake. This ensures that the upscaling stages are grounded on their inputs, i.e that  $\mathbf{x}^l$  "matches" its corresponding  $\mathbf{x}^{l-1}$ .

**Partial View Training** Computational requirements for upscaling levels can be high when generating large outputs. As we increase the length and resolution of a generation, the need to store activation tensors during training increases the amount of GPU memory required. To further reduce the computational requirements, we propose to train the upscaling levels on only temporal crops of their inputs. This strategy reduces training costs since we upscale smaller tensors, at the expense of having less available context to interpolate frames. We define convolutional upscaling levels that learn functions that can be applied in a sliding window manner over their inputs. At inference time, we do not crop the inputs and CVG is applied to all possible input windows, thus generating full-length videos.

## III. MODEL PARAMETRIZATION

In this section we describe the parametrization of the different levels of CVG. We keep the discussion at a high level, briefly mentioning the main components of our model. Precise details on the architecture are provided in the appendix.

**First Level** The first level generator stacks units composed by a ConvGRU layer [7], modeling temporal information, and 2D-ResNet blocks that upsample the spatial resolution. Similar to MoCoGAN [8] and DVD-GAN [9], we use a dual discriminator with both a spatial discriminator that randomly samples  $k$  full-resolution frames and discriminates them individually, and a temporal discriminator that processes spatially downsampled but full-length videos.

**Upsampling Levels** The upsampling levels are composed by a conditional generator and three discriminators (spatial, temporal and matching). The conditional generator produces an upsampled version  $\hat{\mathbf{x}}^l$  of a lower resolution video  $\hat{\mathbf{x}}^{l-1}$ . To discriminate samples from real videos, upscaling stages use a spatial and temporal discriminator, as in the first level. Additionally, we introduce a matching discriminator. The goal of the matching discriminator is to ensure that the output is a valid upsampling of the input, and its necessity arises from the model formulation. Without this discriminator, the upsampling generator could learn to ignore the low resolution input video. The conditional generator is trained jointly with the spatial, temporal and matching discriminators.

**Conditional Generator** The conditional generator takes as input a lower resolution video  $\hat{\mathbf{x}}^{l-1}$ , a noise vector  $\mathbf{z}$  and optionally a class label  $y$ , and generates  $\hat{\mathbf{x}}^l$ . Our conditional generator stacks units composed by one 3D-ResNet block and two 2D-ResNet blocks. Spatial upsampling is performed gradually by progressively increasing the resolution of the generator blocks. To condition the generator we add residual

connections [10], [11] from the low-resolution video to the output of each generator unit.

**Matching Discriminator** The matching discriminator uses an architecture like that of the temporal discriminator. It discriminates real or generated input-output pairs. The output is downsampled to the same size as the input, and both tensors are concatenated on the channel dimension. A precise description of all discriminator architectures can be found in the appendix.

#### IV. RELATED WORK

The modern video generation literature [12], [13] first started as a result of adapting techniques for language modeling to video. Since then, many papers have proposed different approaches to represent and generate videos [14]–[18], including different kinds of tasks, conditionings and models. We review the most common types of generative video models below.

Autoregressive models [19]–[24] model the conditional probability of each pixel value given the previous ones. They do not use latent variables and their training can be easily parallelized. Inference in autoregressive models often requires a full forward pass for each output pixel, which does not scale well to long high resolution videos. Normalizing flows [25]–[27] learn bijective functions that transform latent variables into data samples. Normalizing flows are able to directly maximize the data likelihood. However, they require the latent variable to have the same dimensionality as its output, which becomes an obstacle when generating videos due to their large dimensionality. Variational AutoEncoders (VAEs) [28]–[30] also transform latent variables into data samples. While more scalable, VAEs often produce blurry results when compared to other generative models. Models based on VRNNs [31]–[34] use one latent variable per video frame and often produce better results.

Generative Adversarial Networks (GANs) are also latent variable models and optimize a min-max game between a generator G and a discriminator D trained to tell real and generated data apart [4]. Empirically, GANs usually produce better samples than competing approaches but might suffer from mode collapse. GAN models for video were first proposed in [35]–[37]. In recent work, SAVP [33] proposed to use the VAE-GAN [38] framework for video. TGANv2 [39] improves upon TGAN [40] and proposes a video GAN trained on data windows, similar to our approach. However, unlike TGANv2, our model is composed of multiple stages which are not trained jointly. MoCoGAN [8] first introduced a dual discriminator architecture for video, with DVD-GAN [9] scaling up this approach to high resolution videos in the wild. DVD-GAN outperforms MoCoGAN and TGANv2, and is arguably the current state-of-the-art in adversarial video generation. Our model is also related to work that proposes hierarchical or progressive training approaches for generative models [41]–[44]. Our model is different in that our stages are trained greedily in separate steps without backpropagation from one stage to the other, which reduces its computational requirements.

#### V. EXPERIMENTS

In this section we empirically validate our proposed approach. First, we show that our approach outperforms or matches the state-of-the-art on Kinetics-600 and UCF101. Then, we analyze the scaling properties of our model in Section V-D. Finally, we ablate the main components of our model in Section V-E.

##### A. Experimental Setting

**Datasets** We consider the Kinetics-600 [45], [46] and the UCF101 [47] datasets for class conditional video generation. Kinetics-600 is a large scale dataset of Youtube videos depicting 600 action classes. The videos are captured in the wild and exhibit lots of variability. The amount of videos available from Kinetics-600 is constantly changing as videos become unavailable from the platform. We use a version of the dataset collected on June 2018 with around 350K videos. UCF101 contains approximately 13K videos with around 27 hours of video from 101 human action categories. Its videos have camera motion and cluttered backgrounds, and it is a common benchmark in the video generation community.

Additionally, we use the BDD100K dataset [48] for unconditional video generation. BDD100K contains 100k videos showing more than 1000 hours of driving under different conditions. We use the training set split of 70K videos.

For the rest of the section we denote video dimensions by their output resolution  $D \times D$  and number of frames  $F$  as  $F/D \times D$ .

**Evaluation metrics** Defining evaluation metrics for video generation is an open research area. We use metrics from the image generation literature adapted to video. On Kinetics, we report three metrics: i) Inception Score (IS) given by an I3D model [49] trained on Kinetics-400, ii) Frechet Inception Distance on logits from the same I3D network, also known as Frechet Video Distance (FVD) [50], and iii) Frechet Inception Distance on the last layer activations of an I3D network trained on Kinetics-600 (FID). On BDD100K we report FVD and FID as described before, but we omit IS scores as they are not applicable since there are no classes. On UCF101 we report IS scores following the standard setup in the literature.

**Implementation details** All CVG models are trained with a batch size of 512 and using up to 4 nVidia DGX-1. Levels for Kinetics-600 are trained for 300k iterations, while levels for BDD100K and UCF101 are trained for 100k iterations, all with early stopping when evaluation metrics stop improving. We use PyTorch and distribute training across multiple machines using data parallelism. We synchronize the batch norm statistics across workers. We employ the Adam [51] optimizer to train all levels with a fixed learning rate of  $1 \times 10^{-4}$  for G and  $5 \times 10^{-4}$  for D. We use orthogonal initializations for all weights in our model and spectral norm in the generator and the discriminator. More details can be found in the appendix.

**Baselines** As baselines we consider DVD-GAN [9], TGANv2 [39], [40], VideoGPT [24] and MoCoGAN [8]. Comparisons are mostly against DVD-GAN, as the current state-of-the-art model for class-conditional video generation and the only approach that can generate realistic samples on Kinetics-600.



Fig. 2: **Randomly selected CVG 48/128x128 frame samples for Kinetics-600:** These samples were generated by unrolling CVG 12/128x128 to generate 48 frame sequences, 4 times its training horizon. Each row shows frames from the same sample at different timesteps. The generations are temporally consistent and the frame quality does not degrade over time.

TABLE I: **Results on Kinetics-600 128x128** We compare our two-level CVG against the reported metrics for DVD-GAN [9]. Our model is trained on 12-frame windows and matches the performance of the 12-frame DVD-GAN model. Furthermore, the same CVG model is able to generate 48 frames when applied convolutionally over a full-length first level output. In that setup our model also matches the quality of a 48-frame DVD-GAN model, but has significantly lower computational requirements.

Model	Trained on	Evaluated on 12 frames			Evaluated on 48 frames		
		IS ( $\uparrow$ )	FID ( $\downarrow$ )	FVD ( $\downarrow$ )	IS ( $\uparrow$ )	FID ( $\downarrow$ )	FVD ( $\downarrow$ )
DVD-GAN	12/128x128	77.45	<b>1.16</b>	-	N/A	N/A	N/A
DVD-GAN	48/128x128	N/A	N/A	N/A	<b>81.41</b>	28.44	-
2-Level CVG	12/128x128	<b>104.00</b>	2.09	591.90	77.36	<b>14.00</b>	517.21

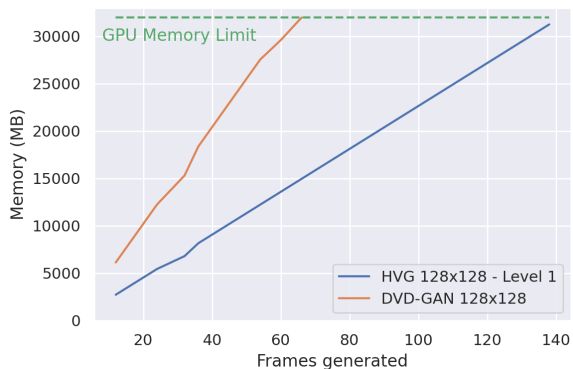


Fig. 3: **Scaling the computational costs** We report the required GPU memory for a two-level CVG. We observe that, given the same batch size, the memory cost scales linearly with the output length. Our model scales better than a comparable non-cascaded model.

### B. Kinetics-600

We first evaluate the performance of CVG on the Kinetics-600 dataset with complex natural videos.

We train a two-level CVG on Kinetics-600 that generates either 12/128x128 or 48/128x128 videos, to compare to the previous state-of-the-art. The first level of CVG generates 24/32x32 videos with a temporal subsampling of 4 frames.

The second level upsamples the first level output using a factor of 2 for the temporal resolution and a factor 4 for the spatial resolution, producing 48/128x128 videos with a temporal subsampling of 2 frames. Since these generations are large, we employ partial views on first level outputs to train the second level, which takes as input windows of 6/32x32 frames and is trained to generate 12/128x128 video snippets (4x lower dimensional than the final output). As a result, this level has approximately the same training cost than a model generating videos of size 12/128x128. At inference time we run the second level convolutionally over all the 24 first level frames to generate 128x128 videos with 48 frames. We also use the same model to generate 12/128x128 videos by using random 6 frame windows from the first level output (i.e. we use the same training and inference setup). We compare to DVD-GAN for both 12/128x128 and 48/128x128 videos with temporal subsampling 2, as the current state-of-the-art in this dataset. Note that DVD-GAN outperforms by a large margin other approaches on Kinetics-600 such as [23].

We report the scores obtained by our model in Table I. For 12/128x128 videos, our model achieves higher IS and comparable FID to DVD-GAN, validating that both models perform comparably when using a similar amount of computational resources. Additionally, CVG outperforms a 48/128x128 DVD-GAN model in FID score and reaches a similar IS score, despite



Fig. 4: **Random 48/256x256 BDD100K samples:** We show samples from our three-stage BDD100K model. Each row shows a different sample over time. Despite the two stages of local upsampling, the frame quality does not degrade noticeably through time.

TABLE II: **UCF101 16/128x128 comparison:** We compare CVG to previous video generation approaches on UCF101. Our method obtains significantly higher Inception Score.

Model	IS(↑)
MoCoGAN [8]	12.42
VideoGPT [24]	24.69
TGANv2 [39]	28.87
DVD-GAN [9]	32.97
CVG (ours)	<b>53.72</b>

only being trained on reduced views of the data. Qualitatively, the generations of both models are similar - they do not degrade noticeable in appearance through time although both have some temporal inconsistencies. For CVG temporal inconsistencies are often due to a poor first level generation. For DVD-GAN we hypothesize that inconsistencies are due to the reduced temporal field of view of its discriminator, which is of less than 10 frames while the model has to generate 48 frames.

### C. UCF101

We further evaluate our approach on the smaller UCF101 dataset. We train a two-level CVG to generate 16/128x128 videos, as commonly done in the literature. The first level generates 8/64x64 videos with a temporal subsampling of 2 frames. The second level upscales the output of the first level to 16/128x128 videos, without temporal subsampling to match the literature. Since these are small videos, we do not use temporal windows to train the second upscaling level.

We report the scores obtained by our model in Table II. Our model obtains state-of-the-art results, outperforming previous approaches by a large margin. Qualitatively, CVG generates coherent samples with high fidelity details, with small temporal inconsistencies. Samples for the UCF101 dataset can be found in the appendix.

### D. Scaling up CVG on BDD100K

To show that our model scales well with the video dimensionality, we train a three-stage model on the BDD dataset

to generate 48/256x256 videos. A training iteration with a single 48/256x256 video for a similarly sized non-cascaded model requires more than 32GB of GPU memory. Such model is therefore not trainable on most current GPUs without techniques like gradient checkpointing which add a significant overhead to the training time. Instead, with our cascaded model we can fit 4 examples per GPU without any engineering tricks.

We train the first level to output 12 frames at 64x64 resolution with a temporal subsampling of 8 frames. The second level upsamples 12 frame windows at 128x128 resolution with temporal subsampling of 4 frames (since we are doubling the framerate of the first level). The third level is trained to upscale 12 frame windows at 256x256 resolution for a final temporal subsampling of 2 frames. Figure 4 shows samples from this model. The videos appear crisp, show multiple settings and do not degrade through time.

To further illustrate the scaling capabilities of our model, we report the memory requirements for a two-level 128x128 CVG as a function of the number of output frames in Figure 3. The first level generates half the output frames at 64x64, while the second level is trained to upscale windows of 6 frames into 12 128x128 frames, regardless of the first level output length. Compared to a non-cascaded 128x128 model, our first level scales better due to the lower resolution and reduced number of frames, and the second level has a fixed memory cost of 10290MB since it is trained on 6 frames windows. Given the same GPU memory budget, our model can generate sequences of up to 140 frames, more than double the frames of a non-cascaded model.

### E. Model Ablations

**Matching Discriminator Ablation** To assess the importance of the matching discriminator, we compare two-level CVG models with and without the matching discriminator (we refer to the latter as No MD). As in Section V-B, we generate 48 frames with a two-level model on Kinetics-600. We train the upscaling level on 3-frame windows of the first level to generate 6 frames. We expect the No MD model to generate



Fig. 5: **Matching discriminator samples** We show a random sample from our two-level model on Kinetics-600 with the matching discriminator and without the matching discriminator (No MD). For each sample we show the output of the first level and the corresponding second level output. While the No MD model generates plausible local snippets at level 2, it does not remain temporally coherent. Our model with the matching discriminator is temporally consistent because it is grounded in the low resolution input.

TABLE III: **Matching discriminator comparison** We report metrics on Kinetics-600 and BDD100K for our model with and without the matching discriminator. Both models perform similarly for 6 frames, corresponding to the training video length. However, the model without the matching discriminator produces incoherent generations when applied over the full first level input because it can ignore it.

Dataset	Model	6 Frames			50 Frames		
		IS ( $\uparrow$ )	FID ( $\downarrow$ )	FVD ( $\downarrow$ )	IS ( $\uparrow$ )	FID ( $\downarrow$ )	FVD ( $\downarrow$ )
Kinetics-600	CVG (No MD)	<b>50.31</b>	1.62	594.99	37.81	42.29	1037.79
	CVG	48.44	<b>1.06</b>	<b>565.95</b>	<b>49.44</b>	<b>31.87</b>	<b>790.97</b>
BDD100K	CVG (No MD)	N/A	1.36	211.69	N/A	26.52	575.51
	CVG	N/A	<b>1.07</b>	<b>144.96</b>	N/A	<b>18.73</b>	<b>326.78</b>

inconsistent full-length videos when applied over the full first level since its outputs are not necessarily valid upscalings of the inputs. On 6 frame generations (i.e. the training setup), CVG and CVG No MD obtain similar scores as reported in Table III. While the No MD model ignores its previous level inputs, it still learns to generate plausible 6 frame videos at 128x128. However, when we use the models to generate full-length 48 frame videos, CVG No MD only generates valid local snippets and is inconsistent through time. Fig. 5 shows an example of a full length No MD generation in which this effect is observable. In contrast, our model (MD) stays grounded to the input and remains consistent through time. This is reflected in the reported metrics in Table III, where the No MD model has worse scores. This ablation shows the need of a matching discriminator to ground upsampling level outputs to their inputs.

**Temporal Window Ablation** One modelling choice in CVG is the temporal window length used in the upsampling levels. Shorter inputs provide less context to upsample frames, while longer inputs require more compute. To assess the impact of the window length, we compare two-level models trained on Kinetics-600 128x128: one trained on first level windows of 6 frames (same setup as in Section V-B) and one trained on windows of only 3 frames. The 6-frame level requires approximately 2x GPU memory than the 3-frame level during training, but we expect it to perform better due to the larger context available for upscaling. We compare their performance

TABLE IV: **Temporal Window Ablation** We compare two-level models trained with different window sizes for the upsampling levels. The 6-frame model has higher computational requirements but outperforms the 3-frame model, confirming a trade-off between computational savings and final performance when selecting the temporal window size.

Window	Kinetics-600 48 Frames		
	IS ( $\uparrow$ )	FID ( $\downarrow$ )	FVD ( $\downarrow$ )
3-frame	58.21	31.59	714.74
6-frame	<b>77.36</b>	<b>14.00</b>	<b>517.21</b>

to generate 48 frames in Table IV. We conclude that the window size defines a trade-off between computational resources and sample quality. We refer the reader to the appendix for an additional ablations and experiments.

## VI. CONCLUSIONS

We propose CVG, a cascaded video generator that divides the generative process into simpler steps. Our model is competitive with state-of-the-art approaches in terms of sample quality, while requiring significantly less computational resources due to the cascaded approach. Higher capacity models and larger outputs are key aspects in improving video generation, and CVG is a step in that direction with better scaling properties than previous approaches.

## Acknowledgements

We thank the Mila Quebec AI Institute for managing the computer clusters on which this research was conducted. This work was supported by an IVADO PhD Fellowship to L.C. and funding from CIFAR.

## REFERENCES

- [1] A. Brock, J. Donahue, and K. Simonyan, "Large scale gan training for high fidelity natural image synthesis," *arXiv preprint arXiv:1809.11096*, 2018. 1
- [2] T. B. Brown, B. Mann, N. Ryder, M. Subbiah, J. Kaplan, P. Dhariwal, A. Neelakantan, P. Shyam, G. Sastry, A. Askell *et al.*, "Language models are few-shot learners," *arXiv preprint arXiv:2005.14165*, 2020. 1
- [3] P. J. Locher, "How does a visual artist create an artwork," *The Cambridge handbook of creativity*, pp. 131–144, 2010. 1
- [4] I. Goodfellow, J. Pouget-Abadie, M. Mirza, B. Xu, D. Warde-Farley, S. Ozair, A. Courville, and Y. Bengio, "Generative adversarial nets," in *Advances in neural information processing systems*, 2014, pp. 2672–2680. 2, 3
- [5] V. Dumoulin, I. Belghazi, B. Poole, O. Mastropietro, A. Lamb, M. Arjovsky, and A. Courville, "Adversarially learned inference," *arXiv preprint arXiv:1606.00704*, 2016. 2
- [6] J. Donahue, P. Krähenbühl, and T. Darrell, "Adversarial feature learning," *arXiv preprint arXiv:1605.09782*, 2016. 2
- [7] N. Ballas, L. Yao, C. Pal, and A. Courville, "Delving deeper into convolutional networks for learning video representations," *arXiv preprint arXiv:1511.06432*, 2015. 2
- [8] S. Tulyakov, M.-Y. Liu, X. Yang, and J. Kautz, "Mocogan: Decomposing motion and content for video generation," in *Proceedings of the IEEE conference on computer vision and pattern recognition*, 2018, pp. 1526–1535. 2, 3, 5
- [9] A. Clark, J. Donahue, and K. Simonyan, "Efficient video generation on complex datasets," *arXiv preprint arXiv:1907.06571*, 2019. 2, 3, 4, 5
- [10] K. He, X. Zhang, S. Ren, and J. Sun, "Deep residual learning for image recognition," in *CVPR*, 2016. 3
- [11] R. K. Srivastava, K. Greff, and J. Schmidhuber, "Highway networks," *arXiv preprint arXiv:1505.00387*, 2015. 3
- [12] M. Ranzato, A. Szlam, J. Bruna, M. Mathieu, R. Collobert, and S. Chopra, "Video (language) modeling: a baseline for generative models of natural videos," *arXiv preprint arXiv:1412.6604*, 2014. 3
- [13] N. Srivastava, E. Mansimov, and R. Salakhudinov, "Unsupervised learning of video representations using lstms," in *International conference on machine learning*, 2015, pp. 843–852. 3
- [14] P. Luc, N. Neverova, C. Couprie, J. Verbeek, and Y. LeCun, "Predicting deeper into the future of semantic segmentation," in *Proceedings of the IEEE International Conference on Computer Vision*, 2017, pp. 648–657. 3
- [15] P. Luc, C. Couprie, Y. Lecun, and J. Verbeek, "Predicting future instance segmentation by forecasting convolutional features," in *Proceedings of the European Conference on Computer Vision (ECCV)*, 2018, pp. 584–599. 3
- [16] R. Villegas, J. Yang, S. Hong, X. Lin, and H. Lee, "Decomposing motion and content for natural video sequence prediction," *arXiv preprint arXiv:1706.08033*, 2017. 3
- [17] R. Villegas, J. Yang, Y. Zou, S. Sohn, X. Lin, and H. Lee, "Learning to generate long-term future via hierarchical prediction," in *Proceedings of the 34th International Conference on Machine Learning-Volume 70*. JMLR. org, 2017, pp. 3560–3569. 3
- [18] T. Xue, J. Wu, K. Bouman, and B. Freeman, "Visual dynamics: Probabilistic future frame synthesis via cross convolutional networks," in *Advances in neural information processing systems*, 2016, pp. 91–99. 3
- [19] H. Larochelle and I. Murray, "The neural autoregressive distribution estimator," in *Proceedings of the Fourteenth International Conference on Artificial Intelligence and Statistics*, 2011, pp. 29–37. 3
- [20] L. Dinh, J. Sohl-Dickstein, and S. Bengio, "Density estimation using real nvp," *arXiv preprint arXiv:1605.08803*, 2016. 3
- [21] N. Kalchbrenner, A. van den Oord, K. Simonyan, I. Danihelka, O. Vinyals, A. Graves, and K. Kavukcuoglu, "Video pixel networks," in *Proceedings of the 34th International Conference on Machine Learning-Volume 70*. JMLR. org, 2017, pp. 1771–1779. 3
- [22] S. Reed, A. van den Oord, N. Kalchbrenner, S. G. Colmenarejo, Z. Wang, Y. Chen, D. Belov, and N. de Freitas, "Parallel multiscale autoregressive density estimation," in *Proceedings of the 34th International Conference on Machine Learning-Volume 70*. JMLR. org, 2017, pp. 2912–2921. 3
- [23] D. Weissenborn, O. Täckström, and J. Uszkoreit, "Scaling autoregressive video models," *International Conference on Learning Representations*, 2020. 3, 4
- [24] W. Yan, Y. Zhang, P. Abbeel, and A. Srinivas, "Videogpt: Video generation using vq-vae and transformers," *arXiv preprint arXiv:2104.10157*, 2021. 3, 5
- [25] D. J. Rezende and S. Mohamed, "Variational inference with normalizing flows," *arXiv preprint arXiv:1505.05770*, 2015. 3
- [26] D. P. Kingma and P. Dhariwal, "Glow: Generative flow with invertible 1x1 convolutions," in *Advances in Neural Information Processing Systems*, 2018, pp. 10215–10224. 3
- [27] M. Kumar, M. Babaeizadeh, D. Erhan, C. Finn, S. Levine, L. Dinh, and D. Kingma, "Videoflow: A flow-based generative model for video," *arXiv preprint arXiv:1903.01434*, vol. 2, no. 5, 2019. 3
- [28] D. P. Kingma and M. Welling, "Auto-encoding variational bayes," *arXiv preprint arXiv:1312.6114*, 2013. 3
- [29] D. J. Rezende, S. Mohamed, and D. Wierstra, "Stochastic backpropagation and approximate inference in deep generative models," *arXiv preprint arXiv:1401.4082*, 2014. 3
- [30] M. Babaeizadeh, C. Finn, D. Erhan, R. H. Campbell, and S. Levine, "Stochastic variational video prediction," *arXiv preprint arXiv:1710.11252*, 2017. 3
- [31] J. Chung, K. Kastner, L. Dinh, K. Goel, A. C. Courville, and Y. Bengio, "A recurrent latent variable model for sequential data," in *Advances in neural information processing systems*, 2015, pp. 2980–2988. 3
- [32] E. Denton and R. Fergus, "Stochastic video generation with a learned prior," in *International Conference on Machine Learning*, 2018, pp. 1182–1191. 3
- [33] A. X. Lee, R. Zhang, F. Ebert, P. Abbeel, C. Finn, and S. Levine, "Stochastic adversarial video prediction," *arXiv preprint arXiv:1804.01523*, 2018. 3
- [34] L. Castrejon, N. Ballas, and A. Courville, "Improved conditional vrnnns for video prediction," in *Proceedings of the IEEE International Conference on Computer Vision*, 2019, pp. 7608–7617. 3
- [35] C. Vondrick, H. Pirsiavash, and A. Torralba, "Generating videos with scene dynamics," in *Advances In Neural Information Processing Systems*, 2016, pp. 613–621. 3
- [36] —, "Anticipating visual representations from unlabeled video," in *Proceedings of the IEEE Conference on Computer Vision and Pattern Recognition*, 2016, pp. 98–106. 3
- [37] M. Mathieu, C. Couprie, and Y. LeCun, "Deep multi-scale video prediction beyond mean square error," *arXiv preprint arXiv:1511.05440*, 2015. 3
- [38] A. B. L. Larsen, S. K. Sønderby, H. Larochelle, and O. Winther, "Autoencoding beyond pixels using a learned similarity metric," *arXiv preprint arXiv:1512.09300*, 2015. 3
- [39] M. Saito and S. Saito, "Tganv2: Efficient training of large models for video generation with multiple subsampling layers," *arXiv preprint arXiv:1811.09245*, 2018. 3, 5
- [40] M. Saito, E. Matsumoto, and S. Saito, "Temporal generative adversarial nets with singular value clipping," in *ICCV*, 2017. 3
- [41] T. Karras, T. Aila, S. Laine, and J. Lehtinen, "Progressive growing of gans for improved quality, stability, and variation," *arXiv preprint arXiv:1710.10196*, 2017. 3
- [42] E. L. Denton, S. Chintala, R. Fergus *et al.*, "Deep generative image models using a laplacian pyramid of adversarial networks," in *Advances in neural information processing systems*, 2015, pp. 1486–1494. 3
- [43] W. Xiong, W. Luo, L. Ma, W. Liu, and J. Luo, "Learning to generate time-lapse videos using multi-stage dynamic generative adversarial networks," in *Proceedings of the IEEE Conference on Computer Vision and Pattern Recognition*, 2018, pp. 2364–2373. 3
- [44] L. Zhao, X. Peng, Y. Tian, M. Kapadia, and D. N. Metaxas, "Towards image-to-video translation: A structure-aware approach via multi-stage generative adversarial networks," *International Journal of Computer Vision*, 2020. 3
- [45] W. Kay, J. Carreira, K. Simonyan, B. Zhang, C. Hillier, S. Vijayanarasimhan, F. Viola, T. Green, T. Back, P. Natsev *et al.*, "The kinetics human action video dataset," *arXiv preprint arXiv:1705.06950*, 2017. 3

- [46] J. Carreira, E. Noland, A. Banki-Horvath, C. Hillier, and A. Zisserman, "A short note about kinetics-600," *arXiv preprint arXiv:1808.01340*, 2018. [3](#)
- [47] K. Soomro, A. R. Zamir, and M. Shah, "Ucf101: A dataset of 101 human actions classes from videos in the wild," *arXiv preprint arXiv:1212.0402*, 2012. [3](#)
- [48] F. Yu, W. Xian, Y. Chen, F. Liu, M. Liao, V. Madhavan, and T. Darrell, "Bdd100k: A diverse driving video database with scalable annotation tooling," *arXiv preprint arXiv:1805.04687*, 2018. [3](#)
- [49] J. Carreira and A. Zisserman, "Quo vadis, action recognition? a new model and the kinetics dataset," in *CVPR*, 2017, pp. 6299–6308. [3](#)
- [50] T. Unterthiner, S. van Steenkiste, K. Kurach, R. Marinier, M. Michalski, and S. Gelly, "Towards accurate generative models of video: A new metric & challenges," *arXiv preprint arXiv:1812.01717*, 2018. [3](#)
- [51] D. P. Kingma and J. Ba, "Adam: A method for stochastic optimization," *arXiv preprint arXiv:1412.6980*, 2014. [3](#)